Virulence

ISSN: (Print) (Online) Journal homepage: www.tandfonline.com/journals/kvir20

Resveratrol-coated gold nanorods produced by green synthesis with activity against *Candida albicans*

Paulo Henrique Fonseca Do Carmo, Anna Carolina Pinheiro Lage, Maíra Terra Garcia, Newton Soares da Silva, Daniel Assis Santos, Eleftherios Mylonakis & Juliana Campos Junqueira

To cite this article: Paulo Henrique Fonseca Do Carmo, Anna Carolina Pinheiro Lage, Maíra Terra Garcia, Newton Soares da Silva, Daniel Assis Santos, Eleftherios Mylonakis & Juliana Campos Junqueira (2024) Resveratrol-coated gold nanorods produced by green synthesis with activity against *Candida albicans*, Virulence, 15:1, 2416550, DOI: 10.1080/21505594.2024.2416550

To link to this article: https://doi.org/10.1080/21505594.2024.2416550

Published online: 19 Oct 2024.

VIRULENCE
2024, VOL. 15, NO. 1, 2416550
https://doi.org/10.1080/21505594.2024.2416550

Taylor & Francis
Taylor & Francis Group

RESEARCH ARTICLE

OPEN ACCESS Check for updates

Resveratrol-coated gold nanorods produced by green synthesis with activity against *Candida albicans*

Paulo Henrique Fonseca Do Carmo [a*], Anna Carolina Pinheiro Lage [b*], Maíra Terra Garcia [a], Newton Soares da Silva [a], Daniel Assis Santos [c], Eleftherios Mylonakis [d], and Juliana Campos Junqueira [a]

[a]Department of Biosciences and Oral Diagnosis, Institute of Science and Technology, São Paulo State University (Unesp), São José dos Campos, SP, Brazil; [b]Department of Medicine, René Rachou Research Centre, Fiocruz Minas, Belo Horizonte, MG, Brazil; [c]Department of Microbiology, Institute of Biological Sciences, Universidade Federal de Minas Gerais, Belo Horizonte, MG, Brazil; [d]Department of Medicine, Houston Methodist Hospital, Houston, TX, USA

ABSTRACT

Candida albicans is an opportunistic yeast capable of causing a wide range of mucosal, cutaneous, and systemic infections. However, therapeutic strategies are limited to a few antifungal agents. Inorganic nanoparticles have been investigated as carrier systems for antifungals as potential new treatments. In this study, we focused on the antifungal activity of gold nanorods, a specific rod-shaped gold nanoparticle, produced by green synthesis using resveratrol as a metal-reducing agent. The synthesis method resulted in stable control nanoparticles (AuNp) and resveratrol-coated gold nanoparticles (AuNpRSV) with medium sizes of 32.4 × 15.9 nm for AuNp, and 33.5 × 15.3 nm for AuNpRSV. Both AuNp and AuNpRSV inhibited the *C. albicans* grown at 2.46 µg/mL, exhibited fungicidal effects at 4.92 µg/mL, and significantly decreased filamentation, biofilm viability, reactive oxygen species production and ergosterol levels of *C. albicans*. In addition, exposure to AuNpRSV reduced the ability of *C. albicans* to grow in the presence of cell membrane stressors. Transmission electron microscopy revealed enlargement of the cell wall and retraction of the cell membrane after treatment with AuNp and AuNpRSV. Promisingly, *in vivo* toxicity analysis demonstrated that both nanoparticles maintained the full viability of *Galleria mellonella* larvae at 49.20 µg/mL. In conclusion, both gold nanoparticles exhibited antifungal activity; however, these effects were enhanced by AuNpRSV. Altogether, AuNps and AuNpRSVs are potential antifungal agents for the treatment of *C. albicans* infections.

ARTICLE HISTORY
Received 20 December 2023
Revised 7 June 2024
Accepted 5 September 2024

KEYWORDS
Gold nanoparticles; Biofilm; Ergosterol; Filamentation; Reactive oxygen species

Introduction

Candida albicans is an opportunistic yeast that colonizes the oral cavity, skin, gastrointestinal tract, and reproductive tract in approximately 50% of healthy individuals [1,2]. Alterations in the host immune response, changes in the resident microbiota, and other factors can lead to *C. albicans* overgrowth, resulting in a wide range of infections [3]. The pathogenicity of *C. albicans* is associated with hyphal formation, secretion of proteolytic enzymes, haemolytic activity, and biofilm formation [4,5]. The ability to form biofilms on host tissue surfaces, medical devices, and dental prostheses is considered one of the most important virulence factors of *C. albicans* [6,7]. Biofilm structure protects *C. albicans* cells from antifungal therapies [8,9] and impairs treatment success [8,10].

C. albicans infections are usually treated with polyenes, azoles, and echinocandins [11]. However, these antifungal agents have limitations in terms of toxicity, recalcitrance, route of administration, high cost, and resistance [4,12,13]. To overcome these limitations, new therapeutic strategies are under investigation. One of these strategies involves studying the antifungal activity of polyphenols and the use of carrier systems [14–17].

Polyphenols are natural organic compounds with one or more phenolic groups of low molecular weight that exhibit anticancer, anti-inflammatory, antioxidant, and antimicrobial activities [18,19]. Previous studies have shown that resveratrol inhibits the planktonic and biofilm growth of *C. albicans* [16,20]. Among carrier systems, gold nanoparticles have been widely studied because of their adjustable physicochemical properties and the potential to deliver antifungal compounds [21–23]. Additionally, gold nanoparticles can have a multi-target mode of action, which may reduce the occurrence of antifungal resistance [15,24].

CONTACT Anna Carolina Pinheiro Lage anna.lage@fiocruz.br
*Both authors contributed equally and shared first authorship.

Recently, green synthetic methods have emerged as innovative approaches for the production of metal nanoparticles. Green synthesis employs compounds of natural origin (plant or microorganism extracts) to reduce metal ions and obtain more stable nanoparticles [25]. Green synthesis is an eco-friendly and sustainable approach that uses an environmentally favourable solvent system instead of toxic reducing agents. Some studies have investigated the effects of gold nanoparticles produced by green synthesis on *C. albicans*. Gold nanoparticles associated with olive leaf extract inhibited the planktonic growth of *C. albicans* and showed enhanced activity compared to the antifungal nystatin [26]. In a separate study, Judan et al. [27] synthesized gold nanoparticles using extracts from 15 ethnobotanicals and observed their ability to reduce biofilm formation by *C. albicans* [15,24].

Since resveratrol is considered a bioactive compound against *C. albicans* and gold nanoparticles are an effective carrier system for antifungal agents, in this study, we employed resveratrol to produce green gold rod-shaped nanoparticles. Control gold nanoparticles (AuNps) and resveratrol-coated gold nanoparticles (AuNpRSVs) were synthesized and characterized. Their effects were evaluated against planktonic cells, biofilms, and virulence factors of *C. albicans*. Additionally, its mode of action on fungal cells and toxicity in *Galleria mellonella* model were investigated.

Material and methods

Chemicals

The chemicals employed for each assay are described as follow: chloroauric acid ($HAuCl_4$), silver nitrate ($AgNO_3$), cetyltrimethylammonium bromide (CTAB), resveratrol (RSV), and sodium borohydride ($NaBH_4$) for the synthesis of gold nanorods; potassium bromide (KBr) tablets for the infrared spectroscopy; fluconazole (FCZ), amphotericin B (AMB), CTAB and RSV for the susceptibility assay; sodium bicarbonate ($NaHCO_3$) and morpholinopropanesulfonic acid (MOPS) for preparation of RPMI-1640 medium; potassium hydroxide (KOH) and n-heptane for the ergosterol analysis; antifungals AMB, FCZ, and the reagents sodium chloride (NaCl), Congo red (RED), and calcofluor white (CFW) for stressor agents in the spot tests; paraformaldehyde, glutaraldehyde, osmium tetroxide (OsO_4), potassium ferricyanide ($C_6N_6FeK_3$), and calcium chloride ($CaCl_2$) for microscopic analysis.

Green synthesis of gold nanoparticles

Gold nanoparticles were synthesized as described previously [28]. The growth solution was prepared using 50 µL of 0.65 mm $HAuCl_4$, 13 µL of 0.11 mm $AgNO_3$, 50 mm CTAB, and 5 mm RSV (Sigma-Aldrich, St. Louis, MO). Then, 600 µL of 3.0 mm $NaBH_4$ solution was added, and the reaction mixture was heated to 70°C. The gold-to-silver ratio (6:1) was kept constant, and after 4 h, the reaction medium was centrifuged for 20 min at 10,000 × g. Then, the pellet was collected and resuspended in 100 mL distilled water [28]. This process was performed three times to eliminate residues.

Characterization of gold nanoparticles

Ultraviolet-visible spectroscopy

Gold nanoparticles were initially characterized by UV – vis absorption spectroscopy using a Rayleigh VIS 723-G spectrophotometer to confirm the characteristic spectrum. The particles were also characterized in relation to the concentration of Au° using the optical density (O.D.) at 400 nm removed from the spectrum, with a validated mathematical treatment [29,30]. The longitudinal surface plasmonic resonance peak was used to estimate the aspect ratio (AR) [31].

Transmission electron microscopy (TEM)

Transmission electron microscopy (TEM) images were obtained using a Tecnai G2–12 electron microscope (SpiritBiotwin FEI, 120 kV). Size distribution analysis and standard deviation were obtained using Image J software (National Institutes of Health [NIH], Bethesda, MD, USA), using TEM images of at least 100 particles. The data obtained were plotted using OriginPro 8.5 for statistical analysis [28].

Zeta potential

AuNps and AuNpRSVs were characterized by the zeta potential in an Anton Paar Litesizer 500 device, using an electrophoretic mobility cell for the device model [28].

Infrared spectroscopy

Owing to the amphiphilic nature of polyphenols, they can be intercalated with CTAB on the surface of gold nanoparticles when introduced into the synthesis [32,33]. Therefore, through infrared spectroscopy analysis (FTIR), the presence of resveratrol on the surface of gold nanoparticles produced by the seedless method can be evaluated. FTIR spectroscopy was performed using a Shimadzu FTIR 8400 apparatus, and 5 mL of each gold nanoparticle sample was centrifuged, resuspended in 1 mL of Milli-Q water, and lyophilized. Each lyophilized sample was incorporated into KBr tablets and inserted into the device for readings from 4000 to 500 cm^{-1}, with 200 reading accumulations [28].

C. albicans strains

We used two strains of *C. albicans*, a reference strain (*C. albicans* SC5314) and a strain isolated from the oropharyngeal candidiasis of a patient living with HIV (*C. albicans* 60) [34]. These strains were cultured on Sabouraud dextrose agar (SDA; Difco, Detroit, MI, USA) at 37°C for 24 h prior to each assay.

Experimental groups

To study *C. albicans*, control gold nanoparticles (AuNps) and resveratrol-coated gold nanoparticles (AuNpRSV) were evaluated. Prior to each assay, AuNp and AuNpRSV were centrifuged at 3500 × g at 20°C for 30 min. After this period, at least 95% of the supernatant was removed, and the remaining content was transferred to a new tube. Then, the equivalent volume of the removed supernatant was replaced in distilled water. After this, the stock solution was diluted again to reach the concentration of the working solution. The antifungals fluconazole (FCZ; Sigma-Aldrich, St. Louis, MO), amphotericin B (AMB; Sigma-Aldrich), the surfactant CTAB, and the polyphenol RSV were also included as control in the experiments.

Susceptibility of C. albicans planktonic cells to AuNp and AuNpRSV

To determine the susceptibility of *C. albicans* planktonic cells to the gold nanoparticle (AuNp), gold nanoparticle with resveratrol (AuNpRSV), AMB, FCZ and RSV, we employed the broth microdilution method proposed by the Clinical and Laboratory Standards Institute (CLSI) document M27-A3. We used concentrations ranging from 16.00 to 0.01 µg/mL for AMB and FCZ, from 256.00 to 0.25 µg/mL for RSV, from 157.44 to 0.15 µg/mL for AuNp and AuNpRSV. Concentrations ranging from 350 to 0.68 µM of CTAB were tested.

C. albicans cultures previously grown for 24 h at 37°C were suspended in saline, counted using a haemocytometer, and diluted in RPMI-1640 medium (Sigma-Aldrich; with L-glutamine, without glucose and $NaHCO_3$, buffered to pH 7.0 with 0.165 M MOPS) to reach a final concentration of 10^3 cells/mL. Microplates containing 100 µL of 2-fold serial dilutions of AMB, FCZ, RSV, CTAB, AuNp, and AuNpRSV were inoculated with 100 µL of the adjusted inoculum and incubated at 37°C for 48 h. The minimum inhibitory concentration (MIC) was visually determined as the lowest concentration capable of inhibiting 80% of fungal growth for FCZ and 100% for AMB, RSV, CTAB, AuNp, and AuNpRSV. Fungus-free sterility and growth controls were included, and *C. parapsilosis* ATCC 22,019 was used as a quality control.

Additionally, 10 µL was removed from each well without visible growth after the MIC assay, cultured on SDA plates, and incubated for 24 hours at 37°C. The minimum fungicidal concentration (MFC) was determined as the lowest concentration of AuNp and AuNpRSV capable of preventing 100% fungal growth after plating. The compound was considered fungicidal if the MFC/MIC ratio was ≤ 4 and fungistatic if the ratio was > 4 [35].

Time-kill curves

Time-kill experiments were conducted using the RPMI medium as the growth medium. Based on the MIC values, *C. albicans* SC5314 and *C. albicans* 60 (10^3 cells/mL) were exposed to AMB, FCZ, RSV, AuNps, and AuNpRSV at their MIC and 2× MIC. Aliquots were taken at 0, 2, 8, 24, and 48 h after exposure and plated on SDA to determine the colony-forming units (CFU/mL) [36]. Non-treated cells were used as negative controls.

Effects of AuNp and AuNpRSV against mature biofilms of C. albicans

After the antifungal activity of AuNp and AuNpRSV against *C. albicans* planktonic was determined, we evaluated the effects of AuNp and AuNpRSV against mature biofilms. Suspensions of *C. albicans* SC5314 and *C. albicans* 60 were counted using a haemocytometer and adjusted to 10^7 cells/mL. Initially, 100 µL of the standardized suspension was added to microplates containing Yeast Nitrogen Peptone (YNB; Difco) with 100 mm glucose and incubated for 90 min at 37°C with shaking. The supernatant was then removed, and each well was washed twice with PBS to remove non-adherent cells, 200 µL of fresh YNB was added, and the microplates were incubated for 24 h at 37°C with shaking [37]. After this period, fresh YNB containing AuNp and AuNpRSV at 1× MIC, and 5× MIC was added, and the microplates were incubated for 24 h at 37°C. The untreated group was used for each strain. After treatment, the biofilms were disrupted using an ultrasonic homogenizer (Sonopuls HD 2200, Bandelin Electronic, Berlin, Germany) at 50 W for 30 s. The suspension was plated on SDA, and the plates were incubated at 37°C for 24 h to determine the colony-forming units (CFU/mL).

Influence of AuNp and AuNpRSV on C. albicans filamentation

In a 24-well culture plate, 2 mL of deionized water was mixed with 10% foetal bovine serum (FBS) (Sigma-Aldrich) and 100 µL of standardized *C. albicans* SC5314 or *C. albicans* 60 suspensions (10^7 viable cells/mL). Groups were treated with 1× and 5× MIC of AuNp or AuNpRSV,

and a control group treated with PBS was used. The plates were incubated at 37°C for 24 h (5% CO_2), and then 10 µL of the inoculum was transferred to glass slides. The number of blastoconidia and hyphae was determined by averaging the structure counts per field under a light microscope at 400 × magnification. Four fields were analysed for each slide [38].

Effects of AuNp and AuNpRSV in the production of reactive oxygen species (ROS) and ergosterol levels of C. albicans

The endogenous amount of reactive oxygen species (ROS) was measured using a fluorometric assay with a specific probe. *C. albicans* SC5314 and *C. albicans* 60 (10^3 cells/mL) were exposed to AuNPs and AuNpRSV at sub-inhibitory concentrations (½ MIC) diluted in RPMI medium without phenol red. The suspension was incubated for 3 h and 24 h with 2,7-dichlorofluorescein diacetate (10 µM; DCFH-DA; Life Technologies) to quantify ROS [39]. Fluorescence was measured on a fluorimeter (Synergy 2 SL Luminescence Microplate Reader; Biotek) at excitation and emission wavelengths of 485 and 530 nm, respectively.

To determine the effects of AuNp and AuNpRSV on ergosterol levels in *C. albicans*, SDA plates were supplemented with AuNp and AuNpRSV at 1× and 5× the MIC. Then, fungal inoculum (10^8 CFU) was added, and the plates were incubated at 37°C for 24 h. Fungal mass (20.0 mg) was collected, lysed with an ethanolic solution of potassium hydroxide (25% KOH), mixed for 1 min, and incubated in a water bath at 85°C for 1 h. Sterols were extracted by adding a mixture of n-heptane (Sigma-Aldrich) and distilled water (3:1), followed by vigorous homogenization for 3 min. The supernatant was collected and the ergosterol content was determined by spectrophotometry at 282 nm. A calibration curve using an ergosterol standard (Sigma-Aldrich) was constructed and used to calculate the amount of ergosterol (µg/mL) [40].

Effect of exposure of C. albicans to AuNp and AuNpRSV under favorable and stress conditions

Fungal growth was evaluated by spot testing on SDA (favourable control conditions) and SDA supplemented with different stressors. The cell membrane stressors used were AMB (2.00 µg/mL), FCZ (4.00 µg/mL), and sodium chloride (NaCl; 1.00 M). The cell wall stressors used were Congo red (10 µg/mL) and calcofluor white (CFW; 100 µg/mL).

Suspensions of *C. albicans* SC5314 and *C. albicans* 60 (10^8 cells/mL) in RPMI medium were treated with AuNp and AuNpRSV at their MIC values for 24 h. Non-treated groups were also included. After treatment, the suspension was counted using a haemocytometer and adjusted accordingly. Then, 10 µL of *C. albicans* suspension (10^4, 10^3 and 10^2 cells) was placed on drug-free SDA or SDA supplemented with xenobiotics. Petri dishes were incubated at 37°C for 24 h, and fungal growth was photographed [41,42].

Transmission electron microscopy (TEM)

Suspensions of *C. albicans* SC5314 (10^8 cells/mL) in RPMI medium were treated with AuNp or AuNpRSV at their MIC values for 24 h. The untreated group was included as a negative control. Then, *C. albicans* cells were fixed for at least 2 h at room temperature in paraformaldehyde 4.0%, glutaraldehyde 2.5% in cacodylate buffer 0.1 M, pH 7.2. After fixation, cells were washed in PBS and postfixed in OsO_4 1% in cacodylate buffer 0.1 M, pH 7.2 with potassium ferricyanide 1%, and $CaCl_2$ 5 mm at room temperature in the dark. The cells were then washed in PBS, dehydrated in acetone, and embedded in Epon. Thin sections were stained with uranyl acetate and lead citrate and observed under a Tecnai G2 Spirit BioTWIN 120 kV (FEI) Transmission Electron Microscope.

Toxicity of AuNp and AuNpRSV on Galleria mellonella model

The toxicity of AuNp and AuNpRSV was assessed in *Galleria mellonella*. AuNp and AuNpRSV were injected at different concentrations (1×, 10× and 20× MIC) directly into *G. mellonella* haemolymph and monitored for 7 days to generate survival curves. Groups that were not injected and those injected with PBS were included as controls. Ten larvae were used for each group. Larvae were considered dead if they did not respond to touch [43].

Statistical analysis

Data were analysed in the Prism 6 software (GrapPad Inc., San Diego, CA, USA) using analysis of variance (ANOVA), followed by Tukey's test. Values of $p < 0.05$ were considered statistically significant.

Results

Synthesis and characterization of AuNp and AuNpRSV

Both AuNp and AuNpRSV synthesized by the seedless method presented a blue-coloured colloid dispersion (Figure 1a,c). UV-Vis absorption spectroscopy demonstrated the characteristic spectrum of gold nanoparticles with two plasmonic bands. AuNP and AuNpRSV

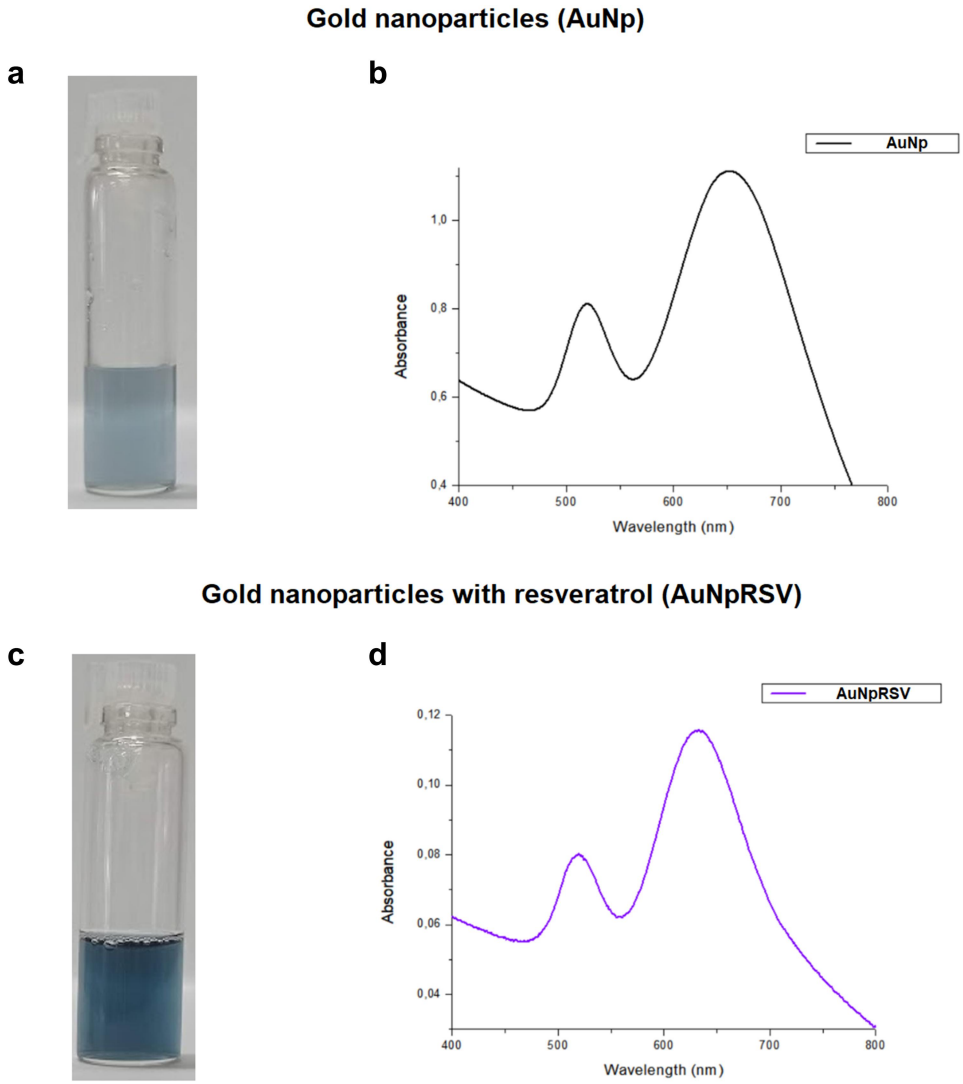

Figure 1. Visual and UV-Vis characteristics of gold nanoparticles. a) aspects and b) UV-Vis spectrum of synthetized of gold nanoparticles (AuNp). c) aspects and d) UV-Vis spectrum of synthetized of gold nanoparticles with resveratrol (AuNpRSV).

exhibited a transverse surface plasmon resonance band between 500–520 nm, and a longitudinal surface plasmon resonance band between 630–650 nm (Figure 1b, d). The theoretical approach revealed an AR value of approximately 2.

TEM images demonstrated rod-shaped gold nanoparticles (Figure 2) and confirmed an AR of approximately 2, which matches the AR acquired in the UV-Vis spectrum.

The medium sizes found were 32.4 ± 3 nm (length) X 15.9 ± 1,8 nm (diameter) for AuNp, and 33.5 ± 1.5 nm (length) X 15.3 ± 1.8 nm (diameter) for AuNpRSV, as shown in sizes distribution histograms (Figure 3).

The infrared spectra of CTAB and free resveratrol (Figure 4a), AuNp and AuNpRSV were determined, verifying that the FTIR spectra of AuNp contained only CTAB on its surface, whereas AuNpRSV contained a mixture of CTAB and RSV.

In the AuNp, we observed stretches at 3017.7 cm^{-1} that refer to the NH bond of CTAB quaternary ammonium group, stretches at 2917.4 and 2849.9 cm^{-1} indicate presence of CH bonds from alkanes group, and 1474.3 cm^{-1} represent – CH_3 stretching at the end of CTAB structure (Figure 4b). In AuNpRSV, we also observed a band at 3243.4 cm^{-1} due to the presence of the hydroxyl O – H group present in RSV. In these spectra, we found characteristic bands of the aromatic polyphenolic skeleton (stretch C – C) in the region of 1600 to 1400 cm^{-1}, different bands referring to the vibration of the C – H group (1300 to 1000 cm^{-1}), and a C – O connection stretch close to 1200.0 cm^{-1}, indicating the presence of RSV on AuNpRSV produced

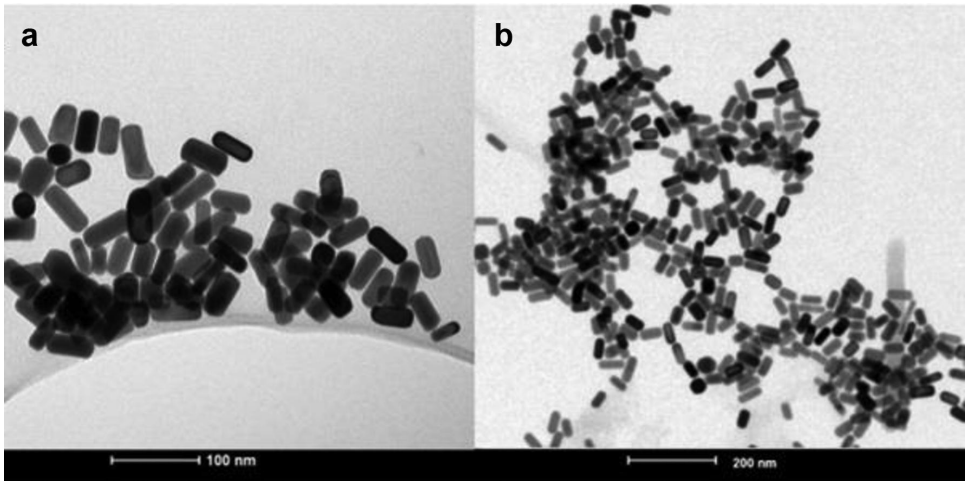

Figure 2. The gold nanoparticles were rod-shaped. TEM images of (a) gold nanoparticles (AuNp) and (b) gold nanoparticles with resveratrol (AuNpRSV).

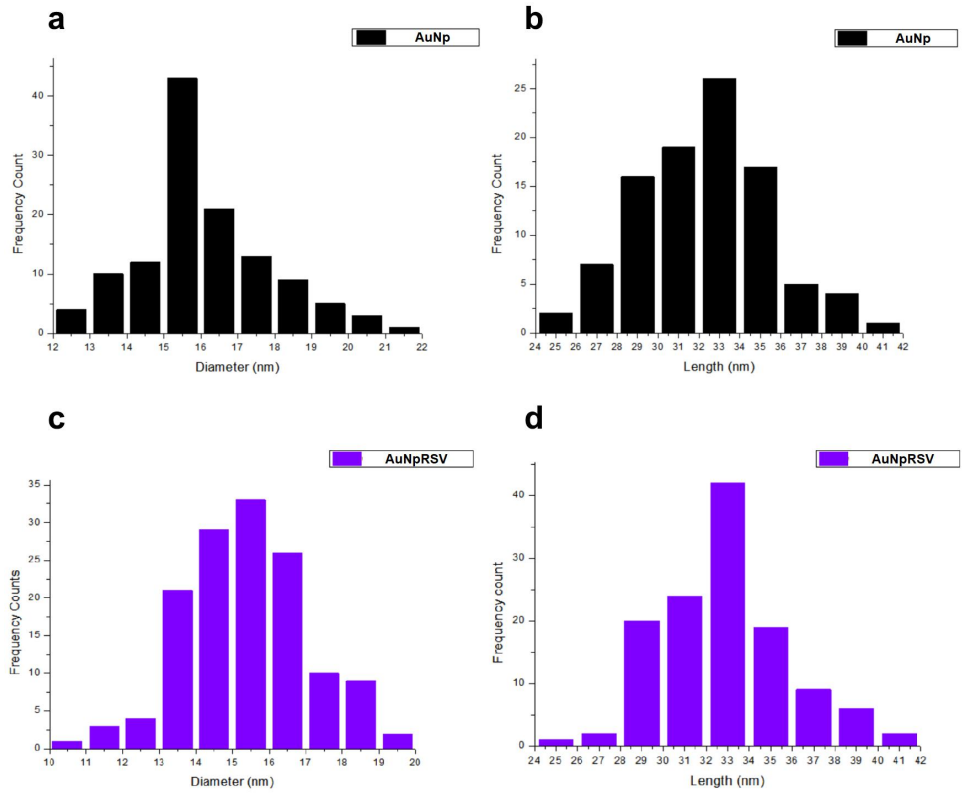

Figure 3. Gold nanoparticles have similar sizes. Histograms of size distribution (diameter and length) of a and b) gold nanoparticles (AuNp), and c and d) gold nanoparticles with resveratrol (AuNpRSV).

by the seedless method and the exclusive presence of CTAB on AuNps (Figure 4c).

Zeta potential values also confirmed the differences in AuNp surfaces, indicating the effective presence of RSV in AuNpRSV. Values were + 35 (s.d. 1.6) mV and + 53 (s.d. 2.0) mV for AuNp and AuNpRSV, respectively (Figure 5a,b).

AuNp and AuNpRSV exhibited activity against C. albicans planktonic cells

In the broth microdilution tests, we found MIC values of 2.46 µg/mL for AuNp and AuNpRSV, > 256.00 µg/mL for RSV, 0.50 µg/mL for FCZ, and 0.12 µg/mL for AMB. MIC of CTAB was 5.46 µM for both strains. MFC values were 4.92 µg/mL for AuNp

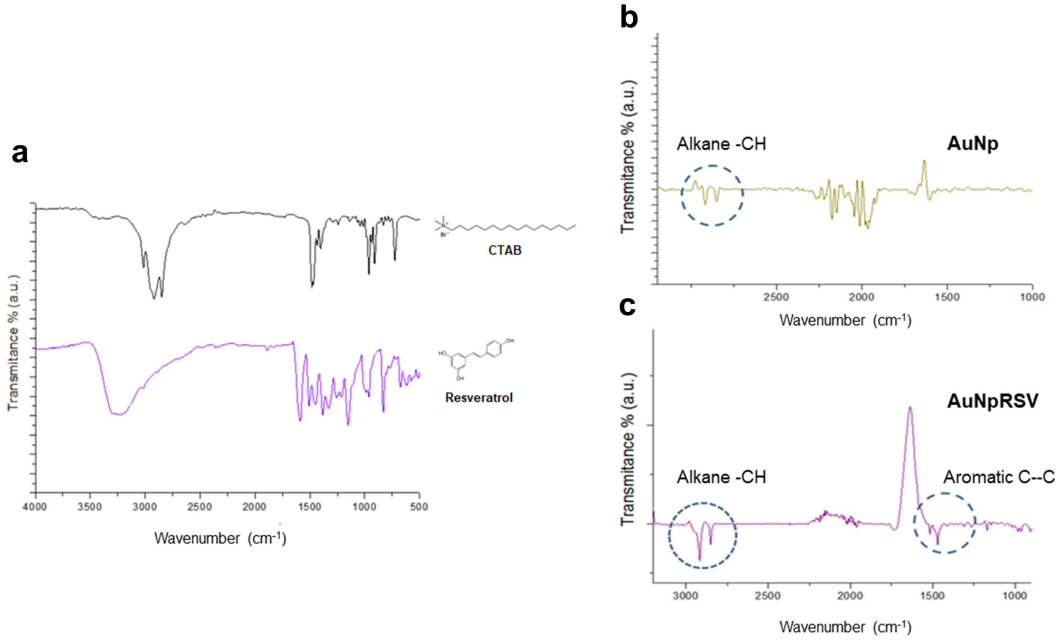

Figure 4. Infrared spectroscopy analysis (FTIR) confirmed synthesis of gold nanoparticles with resveratrol. Infrared spectrum of a) CTAB and free resveratrol, and of b) gold nanoparticles (AuNp) and c) gold nanoparticles with resveratrol (AuNpRSV).

and AuNpRSV, respectively, with an MFC/MIC ratio of 2, indicating fungicidal activity of AuNp and AuNpRSV against *C. albicans* strains (Figure 6a).

We then evaluated the effects of AuNp and AuNpRSV on *C. albicans* viability over time. AuNp (1× MIC) completely decreased the viability of *C. albicans* SC5314 at 24 h and *C. albicans* 60 at 8 h. AuNpRSV (2× MIC) reduced the total viability of both *C. albicans* SC5314 and 60 at 8 h. Microbial reductions remained until the end of the experiment (48 h after treatment) (Figure 6b–e).

AuNp and AuNpRSV decreased viability of mature biofilms and inhibited the filamentation of C. albicans

Based on the *C. albicans* susceptibility results to AuNp and AuNpRSV, we studied their effects on mature biofilms and filamentation ability of *C. albicans*. AuNps significantly reduced the biofilm viability of *C. albicans* SC5314 at 1× MIC and 5× MIC. For *C. albicans* 60, the viability was reduced only at 5× MIC. AuNpRSV significantly decreased the viability of *C. albicans* SC5314 and 60 at both concentrations (Figure 7a,b). In relation to filamentation assays, AuNps reduced the filamentation of both *C. albicans* strains at 1× and 5× MIC. AuNpRSV reduced the number of hyphae at 1× MIC, and completely inhibited filamentation at 5× MIC (Figure 7c,d).

AuNp and AuNpRSV reduced ROS production and ergosterol levels of C. albicans

ROS production decreased significantly with AuNp treatment for *C. albicans* 60 at 2 h and for *C. albicans* SC5314 at 24 h. More specifically, treatment with AuNpRSV reduced ROS for both strains at 2 h and for *C. albicans* SC5314 at 24 h (Figure 8a,b). In relation to ergosterol levels, both AuNp and AuNpRSV treatments reduced the ergosterol content of *C. albicans* SC5314 at 5× MIC, and for *C. albicans* 60 at 1× and 5× MIC. Interestingly, *Candida* cells treated with AuNpRSV had a significantly higher reduction in ergosterol levels than those treated with AuNp (Figure 8c,d).

Exposure to AuNp and AuNpRSV increased the susceptibility of C. albicans to cell membrane and cell wall stressors

As AuNp and AuNpRSV decreased ergosterol levels in *C. albicans*, we studied the effect of AuNp and AuNpRSV exposure on *C. albicans* growth under favourable and stressful conditions. Exposure to AuNps did not affect *C. albicans* SC5314 on SDA, but slightly reduced fungal growth in cell membrane stressors (AMB, FCZ, and NaCl). However, exposure of *C. albicans* SC5314 to AuNpRSV significantly reduced fungal growth on SDA and inhibited growth of both cell membrane and cell wall stressors.

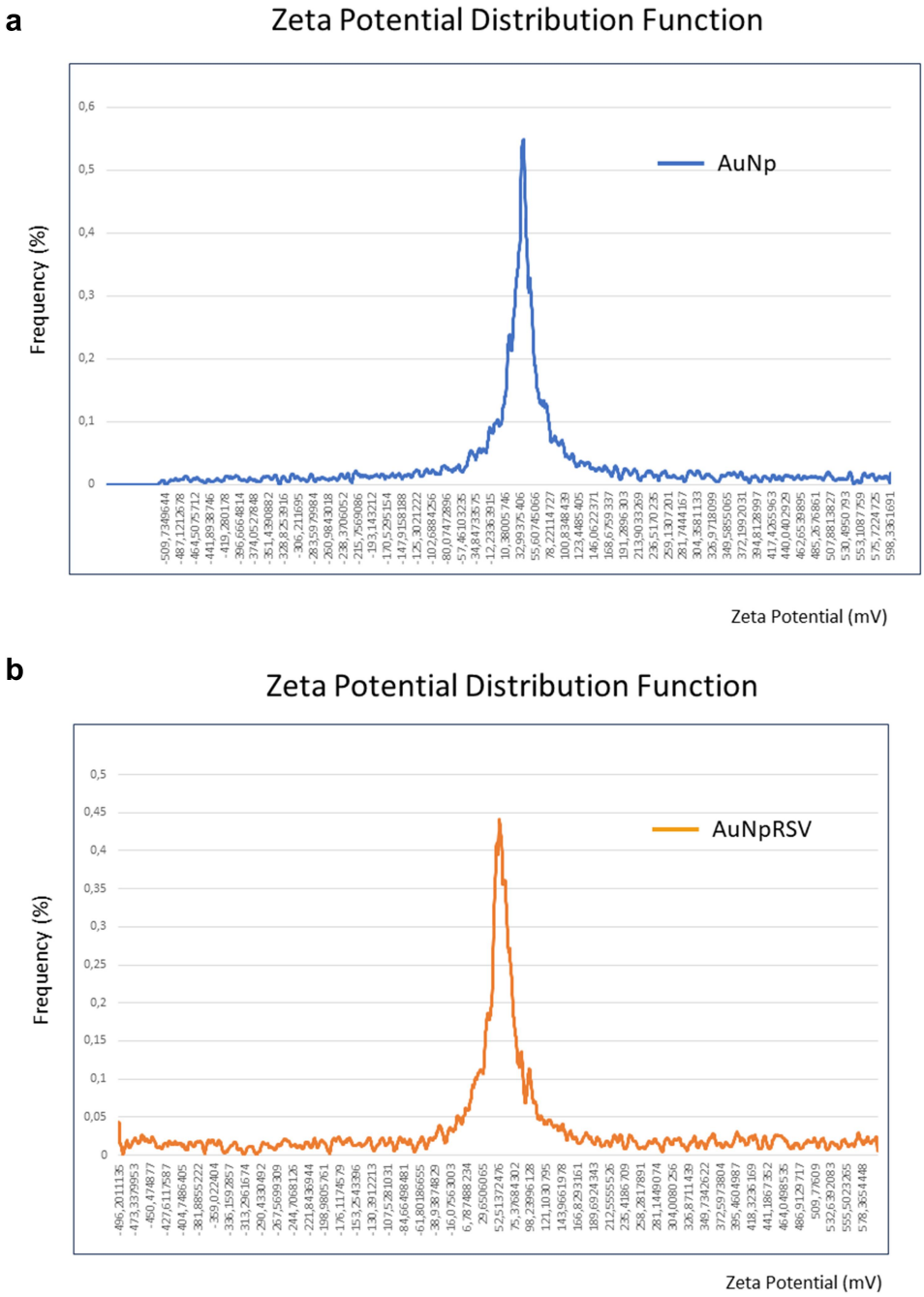

Figure 5. Zeta potential of gold nanoparticles. Zeta potential (mV) of a) gold nanoparticles (AuNp) and b) gold nanoparticles with resveratrol (AuNpRSV).

In relation to *C. albicans* 60, exposure to AuNp reduced cell viability on SDA, as well as on SDA supplemented with cell wall and, mainly, cell membrane stressors (AMB, FCZ, and NaCl). Exposure of *C. albicans* 60 to AuNpRSV decreased the viability of SDA, AMB, RED, and CFW, but the reduction was marked in the FCZ and NaCl stressors (Figure 9).

Exposure to AuNpRSV affected the morphology of C. albicans cells

C. albicans SC5314 cells (non-treated group) displayed well-conserved morphological features with a typical and distinctive membrane and cell wall (Figure 10a). In contrast, cells exposed to AuNps were generally

a

	MIC (µg/mL)					MFC (µg/mL)	MFC/MIC ratio	MFC (µg/mL)	MFC/MIC ratio
Strains	AuNp	RSV	AuNpRSV	AMB	FCZ	AuNp	AuNp	AuNpRSV	AuNpRSV
Candida albicans SC 5314	2.46	> 256.00	2.46	0.12	0.50	4.92	2	4.92	2
Candida albicans 60	2.46	> 256.00	2.46	0.12	0.50	4.92	2	4.92	2
Range	2.46	> 256.00	2.46	0.12	0.50	4.92	2	4.92	2

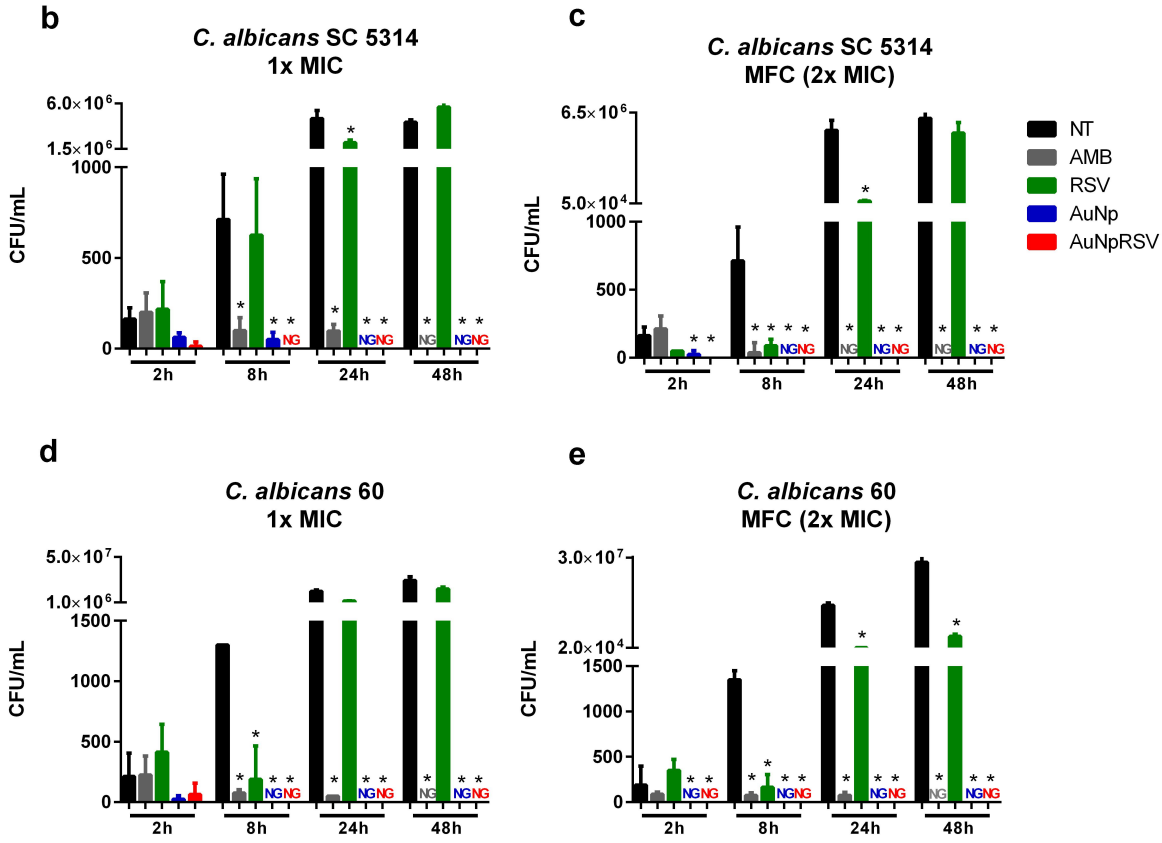

Figure 6. Susceptibility of *C. albicans* strains to AuNp and AuNpRSV. a) minimum inhibitory concentration (MIC), minimum fungicidal concentration (MFC) and MFC/MIC ratio of gold nanoparticles (AuNp), resveratrol (RSV), gold nanoparticles with resveratrol (AuNpRSV), amphotericin b (AMB) and fluconazole (FCZ) against *C. albicans* strains determined by the broth microdilution method. Time-kill curves for *C. albicans* SC 5314 at B) 1× MIC and c) 2× MIC (MFC), and for *C. albicans* 60 at d) 1× MIC and e) 2× MIC (MFC) during 48 hours of treatment. * significant difference compared to non-treated (NT) at each established time ($p < 0.05$). AMB: amphotericin B; AuNp: gold nanoparticles; RSV: resveratrol; AuNpRSV: gold nanoparticles with resveratrol; FCZ: fluconazole; MFC: minimum fungicidal concentration; MIC: minimum inhibitory concentration; NG: no growth; NT: non-treated.

enlarged, with alterations in the cell membrane and cell wall, which showed an increase in thickness and loss of electron-dense characteristics. TEM images also revealed a thin deposition of AuNps, represented by an electrodense line between the cell wall and cell membrane (Figure 10b). Interestingly, exposure to AuNpRSV enhanced cell damage. We observed fungal cells with significant cell wall changes, represented by enlargement and retraction of the cell membrane (Figure 10c). TEM images were used to measure cell wall width. Non-treated fungal cells exhibited a width of 120 nm, whereas cells treated with AuNpRSV were 250 nm in width, confirming the action of AuNpRSV on the cell membrane of *C. albicans*.

AuNp and AuNpRSV maintained full viability of G. mellonella larvae

The survival of *G. mellonella* after inoculation with AuNp or AuNpRSV was determined to assess the

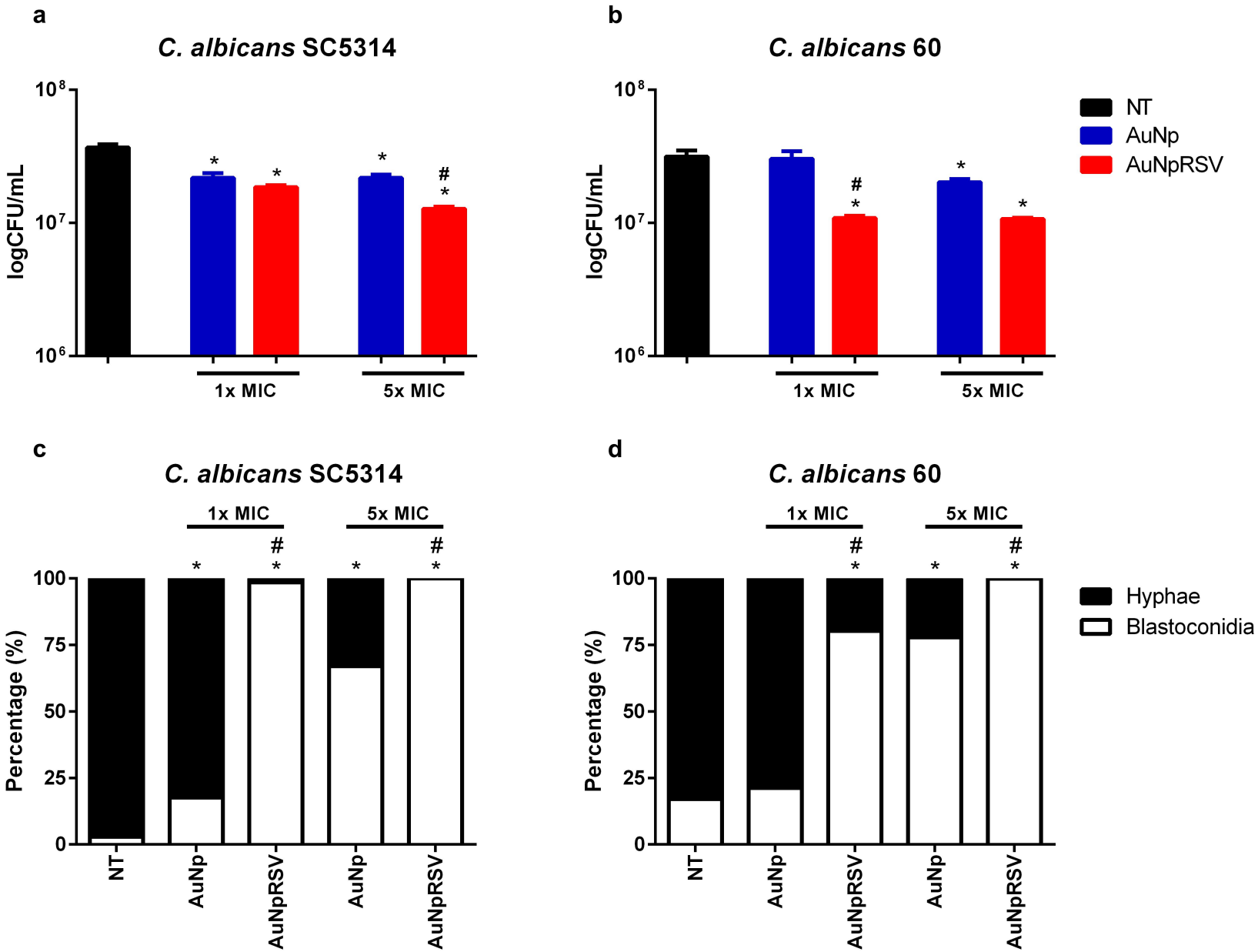

Figure 7. Gold nanoparticles reduced the filamentation and viability of *C. albicans* biofilms. Fungal viability of a) *C. albicans* SC 5314 and b) *C. albicans* 60 biofilms not treated (NT) and treated with gold nanoparticles (AuNp) and gold nanoparticles with resveratrol (AuNpRSV) at 1× and 5× MIC. Percentage of hyphae and blastoconidia of c) *C. albicans* SC 5314 and d) *C. albicans* 60 not treated and treated with AuNp and AuNpRSV at 1× and 5× MIC. *: significant difference compared to non-treated (NT). #: significant difference compared to AuNp ($p < 0.05$). AuNp: gold nanoparticles; AuNpRSV: resveratrol-coated gold nanoparticles; NT: non-treated.

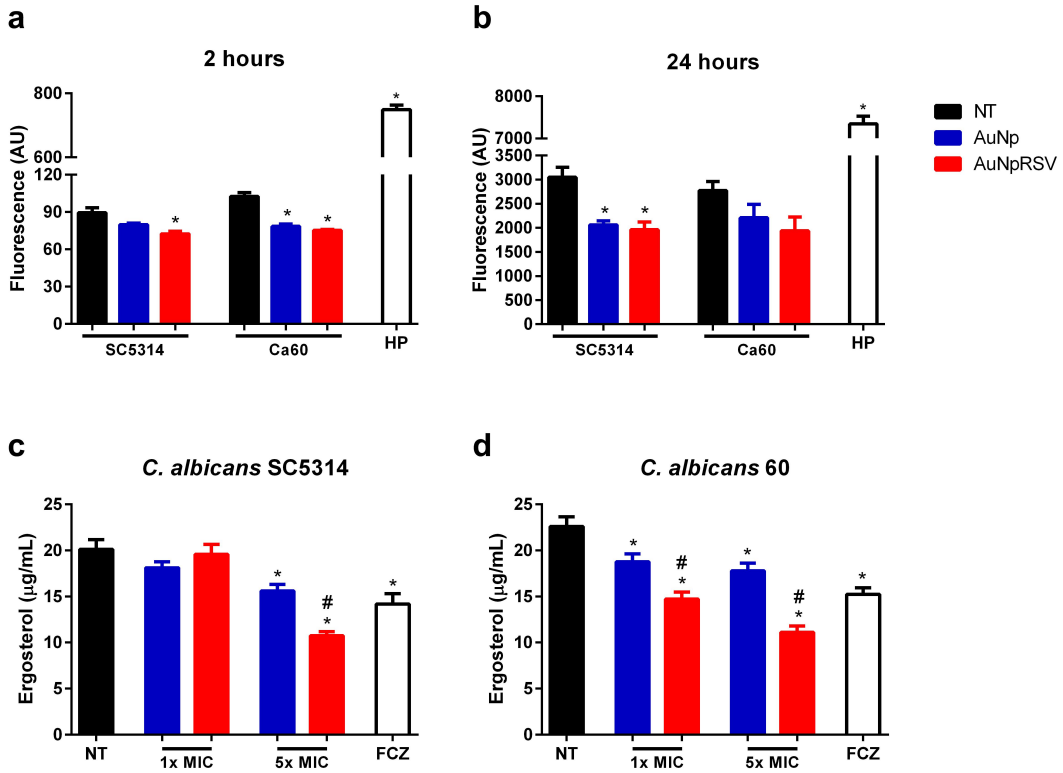

Figure 8. Treatment with gold nanoparticles reduced ROS production and ergosterol levels. Production of reactive oxygen species (ROS) of *C. albicans* SC5314 (SC5314) and *C. albicans* 60 (Ca60) not treated and treated with gold nanoparticles (AuNp), gold nanoparticles with resveratrol (AuNpRSV) and hydrogen peroxide (HP) after a) 2 and b) 24 hours. Ergosterol (µg/mL) levels of c) *C. albicans* SC5314 and d) *C. albicans* 60 not treated (NT) and treated with AuNp and AuNpRSV at 1× and 5× MIC, and with fluconazole (FCZ). *: significant difference compared to non-treated (NT). #: significant difference compared to AuNp ($p < 0.05$). AuNp: gold nanoparticles; AuNpRSV: resveratrol-coated gold nanoparticles; NT: non-treated.

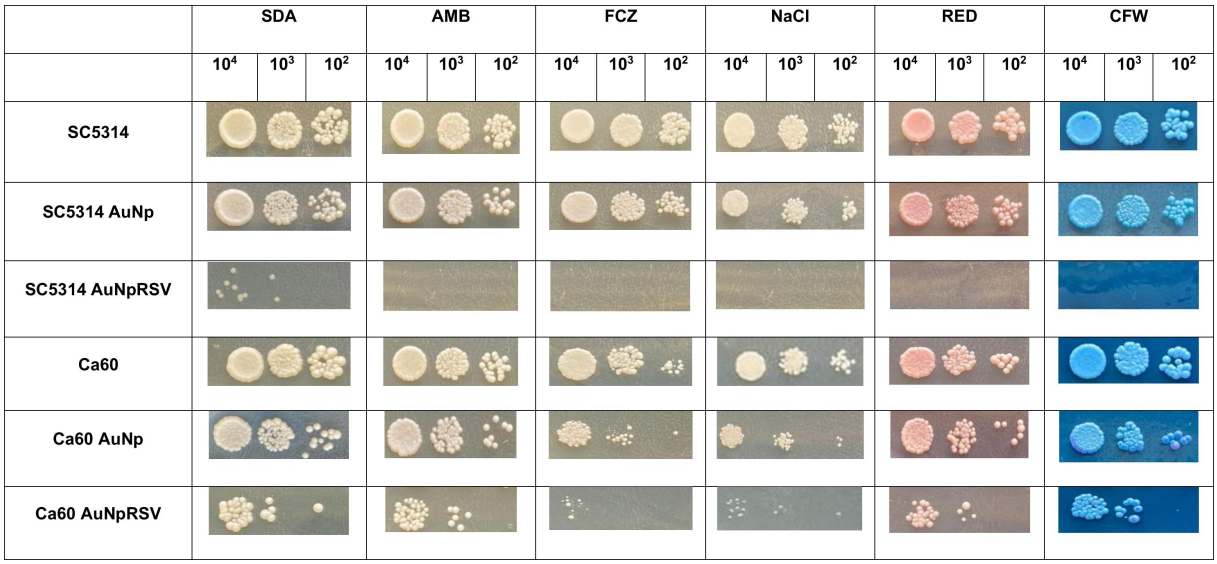

Figure 9. Exposure of *C. albicans* to AuNpRSV affected fungal growth in cell membrane stressors. Spot tests of *C. albicans* SC5314 and *C. albicans* 60 at 10^4, 10^3 and 10^2 cells not exposed and exposed to gold nanoparticles (AuNp) and to gold nanoparticles with resveratrol (AuNpRSV), and plated on sabouraud dextrose agar (SDA) pure, and supplemented with amphotericin B (AMB) fluconazole (FCZ), sodium chloride (NaCl), Congo red (RED) and calcofluor white (CFW).

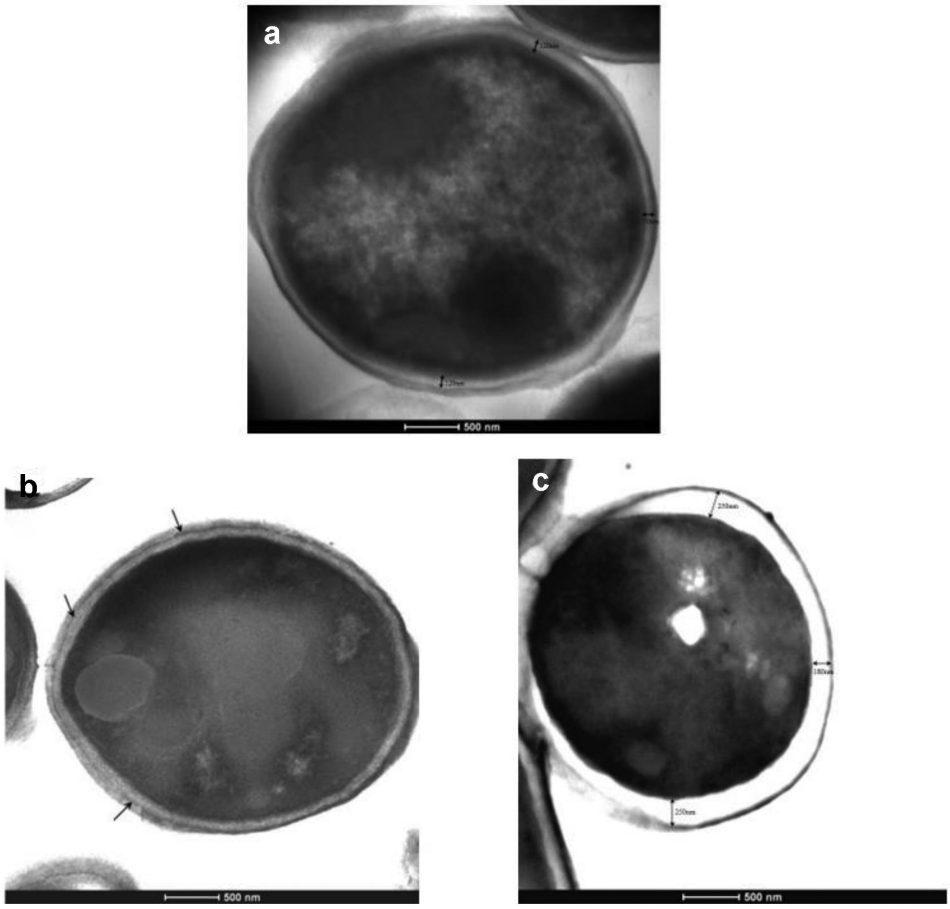

Figure 10. *C. albicans* cell membrane was damaged after exposure to gold nanoparticles. Transmission electronic microscopy (TEM) images of a) cells not treated, and treated with b) gold nanoparticles (AuNp) and c) gold nanoparticles with resveratrol (AuNpRSV). Black arrows indicate a thin deposition of AuNp between of cell membrane and cell wall.

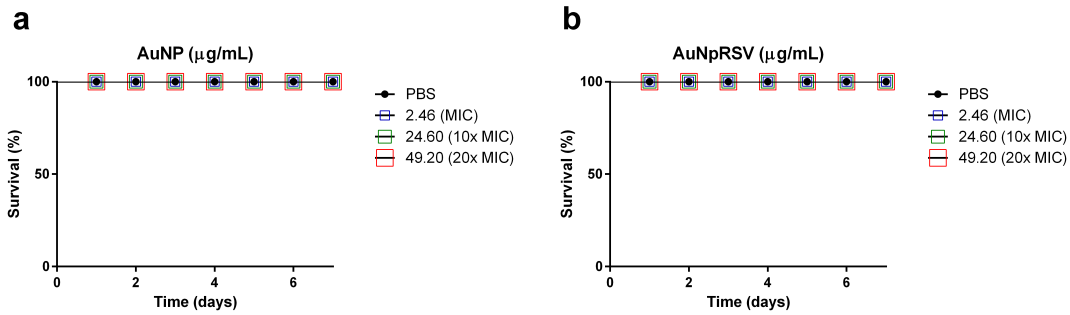

Figure 11. AuNp and AuNpRSV were not toxic to *G. mellonella* larvae. Survival percentage of *galleria mellonella* larvae inoculated with a) gold nanoparticles (AuNp) and b) gold nanoparticles with resveratrol (AuNpRSV) at MIC, 10× MIC and 20× MIC. MIC: minimum inhibitory concentration.

toxicity of the nanoparticles. Both nanoparticles maintained 100% viability of *G. mellonella* larvae at 1×, 10× and even 20× MIC (Figure 11).

Discussion

Gold nanoparticles have been widely studied for the treatment of infectious diseases because of their potential to deliver drugs, including antifungals [21]. Associated with an intrinsic antifungal activity, gold nanoparticles present good physicochemical properties, chemical resistivity, ease of synthesis, and minimal size [44,45].

In this study, we synthesized and characterized gold nanoparticle rod-shaped with resveratrol. Gold atoms tended to be deposited on the tips of the nanostructure

during the growth process, mainly because of the greater binding affinity of CTAB for the lateral facets of the nanostructure. In addition, green synthesis using phenolic compounds, such as RSV, increases the affinity of CTAB for the lateral facets of gold nanorods, facilitating the maintenance of the nanorod structure [46,47]. Although the use of CTAB during the synthesis may be a concern for the biomedical application of nanoparticles [48], washing and dilution processes provide a reduction of this compound to residual concentrations [49], that do not show activity against *C. albicans*.

The synthesis method was successful, according to the characterization data. The seedless method effectively addresses the limitations inherent to conventional approaches, such as variable reproducibility, prolonged reaction times, and inefficient scaling [50,51]. An enhancement strategy for this synthesis method involves the introduction of phenolic compounds, such as resveratrol, as auxiliary reducers. The inclusion of these substances has streamlined particle production, resulting in excellent reproducibility, uniform size characteristics, high yield, and a capacity for large-volume production [28,52]. Moreover, the utilization of resveratrol as a reducing agent aligns with the principles of green synthesis and offers several advantages. This includes the use of reduced amounts of potentially harmful chemicals and production of more stable and monodispersed nanoparticles [49,52,53].

The UV-Vis scanning spectra show the characteristic absorption profiles of AuNp and AuNpRSV, with two distinct plasmon resonance bands. The sizes of the nanoparticles were confirmed using AR analysis and TEM images. Since particle suspensions with zeta potential higher than | 30 | mV is considered stable [54], we obtained good stability for the AuNp (+35 mV) and AuNpRSV (+53 mV) for AuNp and AuNpRSV, respectively. AuNpRSV exhibited a higher zeta potential than AuNp, which confirmed its enhanced colloidal stability. XPs oxygen signals increased significantly in AuNpRSV analysis when compared to AuNp, suggesting the presence of RSV on the nanorods surface, and corroborating the results of the FTIR spectra [28,55]. In addition, both analyzes indicated a low amount of CTAB, mainly in AuNpRSV. Altogether, these data suggest that a good carrier system for RSV was constructed using a green synthesis method [28,56]. The FTIR spectra associated with the XPS data confirmed the presence of RSV on the nanoparticles surfaces [55], suggesting that a good carrier system for RSV was constructed using a green synthesis method [28,56]. Green synthesis is an eco-friendly and inexpensive method that uses natural compounds or microbial metabolites as the reducing and stabilizing agents for gold nanoparticles [25,57]. Furthermore, nanoparticles produced by green synthesis can reduce toxicity [58].

In relation to antifungal activity, we verified that resveratrol was not able to inhibit fungal growth at the highest concentration analysed in this study (256 µg/mL). Indeed, previous studies have demonstrated that concentrations higher than 2000 µg/mL are necessary to reduce fungal growth by 20 % [59,60]. Resveratrol is a phenolic compound present in natural food products, including grapes, wine, peanuts, and berries [61,62]. Furthermore, the low solubility of resveratrol in water and its rapid clearance make it difficult to maintain its bioeffective concentrations in the blood and target tissues of humans [63,64]. Nanoformulation has been proposed as a strategy to overcome the physicochemical limitations of resveratrol [65].

The antifungal effects of AuNps and AuNpRSVs were studied against *C. albicans*. AuNp and AuNpRSV inhibited *C. albicans* growth at 2.46 µg/mL and no fungal burden was detected after 8 h of treatment. In addition, AuNp and AuNpRSV exhibited fungicidal activities against *C. albicans* at low concentrations (4.92 ug/mL). These results indicated that AuNps had an intrinsic effect against *C. albicans* because the MIC and MFC values did not change after functionalization with resveratrol. Ultra Performance Liquid Chromatography (UPLC) analyzes calculated 43.45 µg/mL of RSV on AuNpRSV [49]. However, after the successive washing and dilution processes, probably the final concentration of RSV was minimal. Nevertheless, it contributes to the improved performance of the constructed nanosystem by providing greater stability and enabling synthesis in large volumes.

Nidhin et al. [66] also observed an inhibitory effect of non-functionalized gold nanoparticles against *C. albicans* cells at 0.5 mm. By contrast, Yu et al. [14] found no inhibitory effect of gold nanoparticles (160 ppm) on *C. albicans* growth and hyphal development. In studies with silver nanoparticles (AgNps), Lee et al. [67] and Ahamad et al. [68] demonstrated that treatment of *C. albicans* cells caused a delay in the G1 phase and directly affects the cell cycle. In this phase, the synthesis of RNA, proteins and cellular organelles was observed, that are fundamental structures for fungal replication and growth [69]. Although in our study the growth of *C. albicans* was affected after treatment with AuNp and especially AuNpRSV, the effects of treatment with gold nanoparticles on the cell cycle of *C. albicans* need further investigation.

After the assays in planktonic cells, we studied AuNp and AuNpRSV against mature biofilms and filamentation of *C. albicans*. The ability to change morphology and form biofilms is the chief virulence factor of *C. albicans* and is a central strategy in its pathogenesis [8,70]. Atiencia-Carrera et al. [71] studied the mortality rate in *Candida*-related bloodstream infections and observed that 70% were biofilm-associated. *C. albicans* biofilms are complex structures encapsulated in a self-secreted polymeric extracellular matrix that protects cells from the surrounding environment and provides resistance to conventional antifungal therapy and host immune system components [10,72]. In addition, *C. albicans* forms biofilms on biotic and abiotic surfaces, including host tissues, medical devices, dentures, and catheters, which contribute to recurrent candidiasis and represent a challenge in antifungal therapy [27,70,71]. Therefore, it is important that potential antifungal agents have activity against both the planktonic and biofilm stages of *C. albicans*.

In our study, AuNp reduced biofilm viability and *C. albicans* filamentation at 5× MIC, whereas AuNpRSV decreased viability and filamentation at 1× MIC. Therefore, decreased biofilm viability may be associated with a reduction in the number of hyphae after treatment with gold nanoparticles. Yu et al. showed that non-functionalized gold nanoparticles strongly inhibited *C. albicans* biofilm formation, although no alterations in the expression levels of hypha-specific genes (*HWP1*, *ECE1* and *ALS3)* were detected [14]. In other studies, gold nanoparticles functionalized with fucoidan and β-caryophyllene were able to inhibit polymicrobial biofilms of *C. albicans*, *Staphylococcus aureus* and *Streptococcus mutans* [73], *C. albicans* and *S. aureus*, respectively [74], demonstrating the broad-spectrum antimicrobial activity of gold nanoparticles.

Regarding the effects of AuNp and AuNpRSV on ROS production in *Candida* cells, we observed decreased ROS levels after treatment. Numerous studies have suggested that ROS is intrinsically related to apoptosis in *C. albicans* [39,75,76]. Indeed, ROS are short-lived and highly reactive molecules, and their overexpression causes damage to proteins, nucleic acids, membranes, and organelles, triggering cell death processes including apoptosis [77,78]. This effect was observed by Ahamad et al. [68] and Lee et al. [67] when treating *C. albicans* cells with AgNps. Flow cytometry analyzes revealed that the treatment with AgNps increased cell membrane permeability and reduced the integrity of fungal DNA, resulting in nuclear abnormalities associated with ROS production and apoptosis. However, in this study, we observed reduced ROS production after treatment with AuNp and AuNpRSV, suggesting an ROS-independent apoptotic pathway. Similarly, Seong and Lee [79] demonstrated a pathway in which ROS signalling did not influence the mechanisms of AuNp-induced cell damage. In their study, the mode of action of AuNps was related to DNA damage, mitochondrial dysfunction, and apoptosis via metacaspase activation. However, further investigation is necessary to confirm the mechanism of action of the gold nanorods on ROS production.

In our study, we also verified that AuNp and AuNpRSV reduced ergosterol levels in *C. albicans* cells after treatment with 5× MIC. Interestingly, this reduction was enhanced by treatment with AuNpRSV. Ergosterol is the major sterol in the fungal plasma membrane, contributes to a variety of cellular functions, and is distributed in both the cell membrane and intracellular endomembrane components [80]. Ergosterol is the target of polyene antifungals, and its biosynthetic pathway is the target of allylamines and azole antifungals [81]. However, the effects of resveratrol treatment on *C. albicans* ergosterol levels have not yet been explored. Sun et al. [82] observed that the combination of resveratrol and fluconazole reduced ergosterol levels and increased lanosterol content, a precursor of ergosterol, in *C. albicans*. In addition, studies on other polyphenols, such as honokiol and curcumin, have proven their ability to reduce ergosterol levels in *C. albicans* [80,83].

Interestingly, *C. albicans* cells exposed to AuNpRSV showed a reduced ability to grow on cell membrane stressors (AMB, FCZ, and NaCl), as well as on cell wall stressors (CFW and RED). In contrast, *C. albicans* cells treated with AuNps grew normally in the xenobiotics evaluated. Additionally, TEM images confirmed the interaction of AuNp and AuNpRSV with the cell membrane and revealed significant damage to the treated cells, mainly characterized by enlargement of the cell wall and retraction of the plasma membrane.

Although inorganic nanoparticles exhibit antifungal effects, their cytotoxicity remains a concern [84]. In a previous study by our group [49], AuNps and AuNpRSVs showed reduced cytotoxicity in mammalian cells. The cytotoxic concentrations for 50% of the cells (CC50) were 50 µg/mL and higher than 50 µg/mL for AuNp and AuNpRSV, respectively. We then evaluated the toxicity of both types of nanoparticles using the *G. mellonella* model. This model provides a fast and convenient means of studying *in vivo* toxicity of potential antifungal compounds. In addition, the results showed a strong correlation with the mammalian hosts [85]. In our study, we observed that AuNp and

AuNpRSV did not affect the survival of *G. mellonella* larvae at concentrations up to 49.20 µg/mL, 20 times the MIC value, confirming their reduced toxicity *in vivo*.

In summary, we synthesized and characterized two stable gold nanorods, AuNps and AuRSVs. AuNps exhibited intrinsic activity against planktonic cells and biofilms of *C. albicans*, reducing fungal filamentation, ROS production, and ergosterol levels. However, the antifungal effects of AuNpRSV were enhanced. In addition to its fungicidal activity on *C. albicans* cells and biofilms, treatment with AuNpRSV significantly reduced the levels of ergosterol, and this effect was observed in *C. albicans* cells observed in the TEM images. Importantly, AuNp and AuNpRSV exhibited antifungal effects with no *in vivo* toxicity, reinforcing their potential as agents for treating *C. albicans* infections. These results suggest that the gold nanoparticles produced by green synthesis with resveratrol can be a valuable approach for antifungal therapy against *C. albicans*.

Acknowledgements

We thank Professor Anita Shukla of Brown University for her support. PHFC was supported by the Fundação de Amparo à Pesquisa do Estado de São Paulo – FAPESP (2022/06127-1) and Conselho Nacional de Desenvolvimento Científico e Tecnológico – CNPq (152378/2022-7). JCJ was supported by the FAPESP (2022/15548-0).

Disclosure statement

No potential conflict of interest was reported by the author(s).

Funding

This study was supported by the Fundação de Amparo à Pesquisa do Estado de São Paulo – FAPESP [2022/15548-0 and 2022/06127-1] and Conselho Nacional de Desenvolvimento Científico e Tecnológico – CNPq [152378/2022-7].

Author's Contributions

Conception and design: PHFC, ACPL, JCJ. Methodology: PHFC, ACPL, MTG, NSS, DAS, EM and JCJ. Analysis and interpretation of the data: PHFC, ACP, MTG, NSS, DAS, JCJ. Financial support and supervision: JCJ. Drafting of the paper: PHFC and ACPL. All authors contributed to revision of the manuscript and final approval of the version to be published.

Data availability statement

The data that support the findings of this study are openly available at https://repositorio.unesp.br/items/4645d920-13ee-49ef-b11f-3278b0e81a74.

ORCID

Paulo Henrique Fonseca Do Carmo http://orcid.org/0000-0003-3186-885X
Anna Carolina Pinheiro Lage http://orcid.org/0000-0003-1663-369X
Maíra Terra Garcia http://orcid.org/0000-0002-1193-2909
Newton Soares da Silva http://orcid.org/0000-0001-6452-9278
Daniel Assis Santos http://orcid.org/0000-0002-1108-5666
Eleftherios Mylonakis http://orcid.org/0000-0002-4624-0777
Juliana Campos Junqueira http://orcid.org/0000-0001-6646-6856

References

[1] Nobile CJ, Johnson AD. *Candida albicans* biofilms and human disease. Annu Rev Microbiol. 2015;69(1):71–92. doi: 10.1146/annurev-micro-091014-104330
[2] Talapko J, Juzbašić M, Matijević T, et al. *Candida albicans*—the virulence factors and clinical manifestations of infection. J Fungi. 2021;7(2):79. doi: 10.3390/jof7020079
[3] Vallabhaneni S, Mody RK, Walker T, et al. The global burden of fungal diseases. Infect Dis Clin North Am. 2016;30(1):1–11. doi: 10.1016/j.idc.2015.10.004
[4] Wuyts J, Van Dijck P, Holtappels M, et al. Fungal persister cells: the basis for recalcitrant infections? PlOS Pathog. 2018;14(10):e1007301. doi: 10.1371/journal.ppat.1007301
[5] Cleary IA, Reinhard SM, Lazzell AL, et al. Examination of the pathogenic potential of *C. albicans* filamentous cells in an animal model of haematogenously disseminated candidiasis. FEMS Yeast Res. 2016;fow011. doi: 10.1093/femsyr/fow011
[6] Polívková M, Hubáček T, Staszek M, et al. Antimicrobial treatment of polymeric medical devices by silver nanomaterials and related technology. Int J Mol Sci. 2017;18(2):419. doi: 10.3390/ijms18020419
[7] Jia W, Zhang H, Li C, et al. The calcineruin inhibitor cyclosporine a synergistically enhances the susceptibility of *Candida albicans* biofilms to fluconazole by multiple mechanisms. BMC Microbiol. 2016;16(1):113. doi: 10.1186/s12866-016-0728-1
[8] Gulati M, Nobile CJ. *Candida albicans* biofilms: development, regulation, and molecular mechanisms. Microbes Infect. 2016;18(5):310–321. doi: 10.1016/j.micinf.2016.01.002
[9] Jia D, Sun W. Silver nanoparticles offer a synergistic effect with fluconazole against fluconazole-resistant *Candida albicans* by abrogating drug efflux pumps and increasing endogenous ROS. Infect Genet Evol. 2021;93:104937. doi: 10.1016/j.meegid.2021.104937
[10] Cavalheiro M, Teixeira MC. *Candida* Biofilms: threats, challenges, and promising strategies. Front Med (Lausanne). 2018;5. doi: 10.3389/fmed.2018.00028
[11] Costa-de-Oliveira S, Rodrigues AG. *Candida albicans* antifungal resistance and tolerance in bloodstream infections: the triad yeast-host-antifungal.

Microorganisms. 2020;8(2):154. doi: 10.3390/microorganisms8020154
[12] Peron IH, Reichert-Lima F, Busso-Lopes AF, et al. Resistance surveillance in *Candida albicans*: a five-year antifungal susceptibility evaluation in a Brazilian university hospital. PLOS ONE. 2016;11(7):e0158126. doi: 10.1371/journal.pone.0158126
[13] Stenkiewicz-Witeska JS, Ene IV, Chowdhary A. Azole potentiation in *candida* species. PlOS Pathog. 2023;19(8):e1011583. doi: 10.1371/journal.ppat.1011583
[14] Yu Q, Li J, Zhang Y, et al. Inhibition of gold nanoparticles (AuNPs) on pathogenic biofilm formation and invasion to host cells. Sci Rep. 2016;6(1):26667. doi: 10.1038/srep26667
[15] Salehi Z, Fattahi A, Lotfali E, et al. Susceptibility pattern of Caspofungin-coated gold nanoparticles against clinically important *candida* species. Adv Pharm Bull. 2020;11(4):693–699. doi: 10.34172/apb.2021.078
[16] Okamoto-Shibayama K, Yoshida A, Ishihara K. Inhibitory effect of resveratrol on *Candida albicans* biofilm formation. Bull Tokyo Dent Coll. 2021;62(1):1–6. doi: 10.2209/tdcpublication.2020-0023
[17] Abedini E, Khodadadi E, Zeinalzadeh E, et al. A comprehensive study on the antimicrobial properties of resveratrol as an alternative therapy. Evidence-Based Complement Alternat Med. 2021;2021:1–15. doi: 10.1155/2021/8866311
[18] Manso T, Lores M, de Miguel T. Antimicrobial activity of polyphenols and natural polyphenolic extracts on clinical isolates. Antibiotics. 2021;11(1):46. doi: 10.3390/antibiotics11010046
[19] Fraga CG, Croft KD, Kennedy DO, et al. The effects of polyphenols and other bioactives on human health. Food Funct. 2019;10(2):514–528. doi: 10.1039/C8FO01997E
[20] Vestergaard M, Ingmer H. Antibacterial and antifungal properties of resveratrol. Int J Antimicrob Agents. 2019;53(6):716–723. doi: 10.1016/j.ijantimicag.2019.02.015
[21] Do Carmo PHF, Garcia MT, Figueiredo-Godoi LMA, et al. Metal nanoparticles to combat *Candida albicans* infections: an update. Microorganisms. 2023;11(1):138. doi: 10.3390/microorganisms11010138
[22] Lotfali E, Ghasemi R, Fattahi A, et al. Activities of nanoparticles against fluconazole-resistant *Candida parapsilosis* in clinical isolates. Assay Drug Dev Technol. 2021;19(8):501–507. doi: 10.1089/adt.2021.080
[23] Kumar M, Singh Dosanjh H, Sonika SJ, et al. Review on magnetic nanoferrites and their composites as alternatives in waste water treatment: synthesis, modifications and applications. Environ Sci (Camb). 2020;6(3):491–514. doi: 10.1039/C9EW00858F
[24] Pelgrift RY, Friedman AJ. Nanotechnology as a therapeutic tool to combat microbial resistance. Adv Drug Deliv Rev. 2013;65(13–14):1803–1815. doi: 10.1016/j.addr.2013.07.011
[25] Dikshit P, Kumar J, Das A, et al. Green synthesis of metallic nanoparticles: applications and limitations. Catalysts. 2021;11(8):902. doi: 10.3390/catal11080902
[26] Ayad Kareem H, Mahmood Samaka H, Mohamed Abdulridha W. Evaluation of the gold nanoparticles prepared by green chemistry in the treatment of cutaneous candidiasis. Curr Med Mycol. 2021. doi: 10.18502/cmm.7.1.6176
[27] Judan Cruz KG, Alfonso ED, Fernando SID, et al. Candida albicans biofilm inhibition by ethnobotanicals and ethnobotanically-synthesized gold nanoparticles. Front Microbiol. 2021;12:12. doi: 10.3389/fmicb.2021.665113
[28] Lage ACP, Orlando Ladeira L, Mosqueira L, et al. Synthesis and characterization of gold nanorods using the natural products resveratrol, gallic acid, and a purified fraction of *stryphnodendron obovatum* by seedless method. Environ Nanotechnol Monit Manag [Internet]. 2021;16:100473. Available from: https://www.sciencedirect.com/science/article/pii/S2215153221000489
[29] Hendel T, Wuithschick M, Kettemann F, et al. In situ determination of colloidal gold concentrations with UV–vis spectroscopy: limitations and perspectives. Anal Chem. 2014;86(22):11115–11124. doi: 10.1021/ac502053s
[30] Scarabelli L, Sánchez-Iglesias A, Pérez-Juste J, et al. A "tips and tricks" practical guide to the synthesis of gold nanorods. J Phys Chem Lett. 2015;6(21):4270–4279. doi: 10.1021/acs.jpclett.5b02123
[31] Sprünken DP, Omi H, Furukawa K, et al. Influence of the local environment on determining aspect-ratio distributions of gold nanorods in solution using gans theory. The J Phys Chem C. 2007;111(39):14299–14306. doi: 10.1021/jp074500r
[32] Liopo A, Wang S, Derry PJ, et al. Seedless synthesis of gold nanorods using dopamine as a reducing agent. RSC Adv. 2015;5(111):91587–91593. doi: 10.1039/C5RA19817H
[33] Salavatov NA, Dement'eva OV, Mikhailichenko AI, et al. Some aspects of seedless synthesis of Gold Nanorods. Colloid J. 2018;5:541–549. doi: 10.1134/s1061933x18050149
[34] Junqueira JC, Vilela SFG, Rossoni RD, et al. Oral colonization by yeasts in hiv-positive patients in Brazil. Rev Inst Med Trop S Paulo. 2012;54(1):17–24. doi: 10.1590/S0036-46652012000100004
[35] Hazen KC. Fungicidal versus fungistatic activity of terbinafine and itraconazole: An *in vitro* comparison. J Am Acad Dermatol [Internet]. 1998;38(5):S37–41. Available from doi: 10.1016/S0190-9622(98)70482-7
[36] Scorneaux B, Angulo D, Borroto-Esoda K, et al. SCY-078 is fungicidal against *candida* species in time-kill studies. Antimicrob Agents Chemother. 2017;61(3):61. doi: 10.1128/AAC.01961-16
[37] Rossoni RD, Barbosa JO, de Oliveira FE, et al. Biofilms of *Candida albicans* serotypes A and B differ in their sensitivity to photodynamic therapy. Lasers Med Sci. 2014;29(5):1679–1684. doi: 10.1007/s10103-014-1570-z
[38] Medeiros D, Oliveira-Júnior J, Nóbrega J, et al. Isoeugenol and hybrid acetamides against *Candida albicans* isolated from the oral cavity. Pharmaceuticals. 2020;13(10):291. doi: 10.3390/ph13100291
[39] Li Y, Shan M, Zhu Y, et al. Kalopanaxsaponin a induces reactive oxygen species mediated mitochondrial dysfunction and cell membrane destruction in *Candida albicans*. PLOS ONE. 2020;15(11):e0243066. doi: 10.1371/journal.pone.0243066
[40] Ferreira GF, de Baltazar LM, Santos JRA, et al. The role of oxidative and nitrosative bursts caused by azoles and

amphotericin B against the fungal pathogen *Cryptococcus gattii*. J Antimicrob Chemother. 2013;68 (8):1801–1811. doi: 10.1093/jac/dkt114

[41] Fernandes KE, Dwyer C, Campbell LT, et al. Species in the Cryptococcus gattii complex differ in capsule and cell size following growth under capsule-inducing conditions. mSphere. 2016;1(6):e00350–16. doi: 10.1128/mSphere.00350-16

[42] Carmo PHF, Costa MC, Leocádio VAT, et al. Exposure to itraconazole influences the susceptibility to antifungals, physiology, and virulence of *trichophyton interdigitale*. Med Mycol. 2022;60(11):60. doi: 10.1093/mmy/myac088

[43] de Barros PP, Rossoni RD, Garcia MT, et al. The anti-biofilm efficacy of caffeic acid phenethyl ester (CAPE) *in vitro* and a murine model of oral candidiasis. Front Cell Infect Microbiol. 2021;11:700305. doi: 10.3389/fcimb.2021.700305

[44] Chamundeeswari M, Sobhana SSL, Jacob JP, et al. Preparation, characterization and evaluation of a biopolymeric gold nanocomposite with antimicrobial activity. Biotechnol Appl Biochem. 2010;55(1):29–35. doi: 10.1042/BA20090198

[45] Wani IA, Ahmad T. Size and shape dependant antifungal activity of gold nanoparticles: a case study of *Candida*. Colloids Surf B Biointerfaces. 2013;101:162–170. doi: 10.1016/j.colsurfb.2012.06.005

[46] Alegria E, Ribeiro A, Mendes M, et al. Effect of phenolic compounds on the synthesis of gold nanoparticles and its catalytic activity in the reduction of nitro compounds. Nanomaterials. 2018;8(5):320. doi: 10.3390/nano8050320

[47] Zhang Q, Han L, Jing H, et al. Facet control of gold nanorods. ACS Nano. 2016;10(2):2960–2974. doi: 10.1021/acsnano.6b00258

[48] Wan J, Wang J-H, Liu T, et al. Surface chemistry but not aspect ratio mediates the biological toxicity of gold nanorods in vitro and in vivo. Sci Rep. 2015;5 (1):11398. doi: 10.1038/srep11398

[49] Lage ACP, Ladeira LO, Do Camo PHF, et al. Changes in antiparasitical activity of gold nanorods according to the chosen synthesis. Exp Parasitol. 2022;242:108367. doi: 10.1016/j.exppara.2022.108367

[50] Lai J, Zhang L, Niu W, et al. One-pot synthesis of gold nanorods using binary surfactant systems with improved monodispersity, dimensional tunability and plasmon resonance scattering properties. Nanotechnology. 2014;25(12):125601. doi: 10.1088/0957-4484/25/12/125601

[51] Agrahari K, Rayavarapu RG. Chloride ions assisted synthesis of tunable gold nanorods: seedless synthesis, characterization and *in vitro* toxicity studies. Vacuum. 2019;166:377–384. doi: 10.1016/j.vacuum.2018.10.071

[52] Salavatov NA, Dement'eva OV, Mikhailichenko AI, et al. Some aspects of seedless synthesis of gold nanorods. Colloid J. 2018;80(5):541–549. doi: 10.1134/S1061933X18050149

[53] Chahardoli A, Karimi N, Sadeghi F, et al. Green approach for synthesis of gold nanoparticles from *Nigella arvensis* leaf extract and evaluation of their antibacterial, antioxidant, cytotoxicity and catalytic activities. Artif Cells Nanomed Biotechnol. 2018;46 (3):579–588. doi: 10.1080/21691401.2017.1332634

[54] Jackson SR, McBride JR, Rosenthal SJ, et al. Where's the silver? Imaging trace silver coverage on the surface of gold nanorods. J Am Chem Soc. 2014;136 (14):5261–5263. doi: 10.1021/ja501676y

[55] Silverstein RM, Bassler GC. Spectrometric identification of organic compounds. J Chem Educ. 1962;39 (11):546. doi: 10.1021/ed039p546

[56] Zheng J, Cheng X, Zhang H, et al. Gold nanorods: the most versatile plasmonic nanoparticles. Chem Rev. 2021;121(21):13342–13453. doi: 10.1021/acs.chemrev.1c00422

[57] Różalska B, Sadowska B, Budzyńska A, et al. Biogenic nanosilver synthesized in Metarhizium robertsii waste mycelium extract – as a modulator of Candida albicans morphogenesis, membrane lipidome and biofilm. PLOS ONE. 2018;13(3):e0194254. doi: 10.1371/journal.pone.0194254

[58] Ferreira MD, de Neta LS, Brandão GC, et al. Evaluation of the antimicrobial activity of silver nanoparticles biosynthesized from the aqueous extract of *Schinus terebinthifolius* raddi leaves. Biotechnol Appl Biochem. 2023;70(3):1001–1014. doi: 10.1002/bab.2415

[59] Miyashiro CA, Bernegossi J, Bonifácio BV, et al. Development and characterization of a novel liquid crystalline system containing sodium alginate for incorporation of trans-resveratrol intended for treatment of buccal candidiasis. Pharmazie. 2020;75 (5):179–185. doi: 10.1691/ph.2020.9165

[60] Wang J, Zhang X, Gao L, et al. The synergistic antifungal activity of resveratrol with azoles against *Candida albicans*. Lett Appl Microbiol. 2021;72 (6):688–697. doi: 10.1111/lam.13458

[61] Giovinazzo G, Ingrosso I, Paradiso A, et al. Resveratrol biosynthesis: plant metabolic engineering for nutritional improvement of food. Plant Foods Hum Nutr. 2012;67(3):191–199. doi: 10.1007/s11130-012-0299-8

[62] Lee J, Lee DG. Novel antifungal mechanism of resveratrol: apoptosis inducer in *Candida albicans*. Curr Microbiol. 2015;70(3):383–389. doi: 10.1007/s00284-014-0734-1

[63] Walle T. Bioavailability of resveratrol. Ann N Y Acad Sci. 2011;1215(1):9–15. doi: 10.1111/j.1749-6632.2010.05842.x

[64] Delmas D, Aires V, Limagne E, et al. Transport, stability, and biological activity of resveratrol. Ann N Y Acad Sci. 2011;1215(1):48–59. doi: 10.1111/j.1749-6632.2010.05871.x

[65] Augustin MA, Sanguansri L, Lockett T. Nano- and micro-encapsulated systems for enhancing the delivery of resveratrol. Ann N Y Acad Sci. 2013;1290 (1):107–112. doi: 10.1111/nyas.12130

[66] Nidhin M, Saneha D, Hans S, et al. Studies on the antifungal activity of biotemplated gold nanoparticles over *Candida albicans*. Mater Res Bull. 2019;119:110563. doi: 10.1016/j.materresbull.2019.110563

[67] Lee B, Lee MJ, Yun SJ, et al. Silver nanoparticles induce reactive oxygen species-mediated cell cycle delay and synergistic cytotoxicity with 3-bromopyruvate in *Candida albicans*, but not in *Saccharomyces cerevisiae*.

Int J Nanomedicine. 2019;14:4801–4816. doi: 10.2147/IJN.S205736

[68] Ahamad I, Bano F, Anwer R, et al. Antibiofilm activities of biogenic silver nanoparticles against *Candida albicans*. Front Microbiol. 2022;12:12. doi: 10.3389/fmicb.2021.741493

[69] Chen C, Zeng G, Wang Y. G1 and S phase arrest in *Candida albicans* induces filamentous growth via distinct mechanisms. Mol Microbiol. 2018;110 (2):191–203. doi: 10.1111/mmi.14097

[70] Pereira R, Santos Fontenelle RO, Brito EHS, et al. Biofilm of *Candida albicans*: formation, regulation and resistance. J Appl Microbiol. 2021;131(1):11–22. doi: 10.1111/jam.14949

[71] Atiencia-Carrera MB, Cabezas-Mera FS, Tejera E, et al. Prevalence of biofilms in *Candida* spp. bloodstream infections: a meta-analysis. PLOS ONE. 2022;17(2): e0263522. doi: 10.1371/journal.pone.0263522

[72] Sardi JCO, Scorzoni L, Bernardi T, et al. *Candida* species: current epidemiology, pathogenicity, biofilm formation, natural antifungal products and new therapeutic options. J Med Microbiol. 2013;62(1):10–24. doi: 10.1099/jmm.0.045054-0

[73] Tabassum N, Khan F, Kang M-G, et al. Inhibition of polymicrobial biofilms of *Candida albicans–staphylococcus aureus/Streptococcus mutans* by fucoidan–gold nanoparticles. Mar Drugs. 2023;21(2):123. doi: 10.3390/md21020123

[74] Khan F, Tabassum N, Jeong G-J, et al. Inhibition of mixed biofilms of *Candida albicans* and *staphylococcus aureus* by β-caryophyllene-gold nanoparticles. Antibiotics. 2023;12(4):726. doi: 10.3390/antibiotics12040726

[75] Shahina Z, Ndlovu E, Persaud O, et al. *Candida albicans* reactive oxygen species (ros)-dependent lethality and ROS-Independent hyphal and biofilm inhibition by eugenol and citral. Microbiol Spectr. 2022;10(6):10. doi: 10.1128/spectrum.03183-22

[76] Sun L, Liao K, Hang C, et al. Honokiol induces reactive oxygen species-mediated apoptosis in *Candida albicans* through mitochondrial dysfunction. PLOS ONE. 2017;12 (2):e0172228. doi: 10.1371/journal.pone.0172228

[77] Redza-Dutordoir M, Averill-Bates DA. Activation of apoptosis signalling pathways by reactive oxygen species. Biochim et Biophys Acta (BBA) - Mol Cell Res. 2016;1863(12):2977–2992. doi: 10.1016/j.bbamcr.2016.09.012

[78] Carmo PHF, Freitas GJC, Dornelas JCM, et al. Reactive oxygen and nitrogen species are crucial for the antifungal activity of amorolfine and ciclopirox olamine against the dermatophyte *trichophyton interdigitale*. Med Mycol. 2022;60(8):60. doi: 10.1093/mmy/myac058

[79] Seong M, Lee DG. Reactive oxygen species-independent apoptotic pathway by gold nanoparticles in *Candida albicans*. Microbiol Res. 2018;207:33–40. doi: 10.1016/j.micres.2017.11.003

[80] Sun L, Liao K. The effect of Honokiol on ergosterol biosynthesis and vacuole function in *Candida albicans*. J Microbiol Biotechnol. 2020;30(12):1835–1842. doi: 10.4014/jmb.2008.08019

[81] Odds FC, Brown AJP, Gow NAR. Antifungal agents: mechanisms of action. Trends Microbiol. 2003;11 (6):272–279. doi: 10.1016/S0966-842X(03)00117-3

[82] Sun S, Gao Y, Ling X, et al. The combination effects of phenolic compounds and fluconazole on the formation of ergosterol in *Candida albicans* determined by high-performance liquid chromatography/tandem mass spectrometry. Anal Biochem. 2005;336(1):39–45. doi: 10.1016/j.ab.2004.06.038

[83] Sharma M, Sanjiveeni D, Ashutosh S, et al. Lipidome analysis reveals antifungal polyphenol curcumin affects membrane lipid homeostasis. Front Biosci. 2012;E4 (4):1195. doi: 10.2741/e451

[84] Zhang X, Wu H, Wu D, et al. Toxicologic effects of gold nanoparticles *in vivo* by different administration routes. Int J Nanomedicine. 2010;5:771–781.

[85] Piatek M, Sheehan G, Kavanagh K. *Galleria mellonella*: the versatile host for drug discovery, *in vivo* toxicity testing and characterising host-pathogen interactions. Antibiotics. 2021;10(12):1545. doi: 10.3390/antibiotics10121545